Título:

Low-Cost Solar Irradiance Meter using LDR Sensors

Autores:

R. C. de Barros, J. M. S. Callegari, D. C. Mendonça, W. C. S. Amorim, M. P. Silva e H. A. Pereira.

Publicado em:

13th IEEE/IAS International Conference on Industry Application (Induscon)

Data da Publicação:

2018

Citação para a versão publicada:

R. C. de Barros, J. M. S. Callegari, D. C. Mendonça, W. C. S. Amorim, M. P. Silva and H. A. Pereira, " "Low-Cost Solar Irradiance Meter using LDR Sensors," 13th IEEE/IAS International Conference on Industry Application (Induscon), São Paulo, 2018, pp. 1-8.

Low-Cost Solar Irradiance Meter using LDR Sensors

Rodrigo Cassio de Barros
Department of Electrical Engineering
CEFET - MG
Belo Horizonte, MG, Brazil
rodrigocdebarros@gmail.com

João Marcus Soares Callegari
Department of Electrical Engineering
Federal University of Viçosa - UFV
Viçosa, MG, Brazil
joao.callegari@ufv.br

Dayane do Carmo Mendonça
Department of Electrical Engineering
Federal University of Viçosa - UFV
Viçosa, MG, Brazil
dayane.mendonca@ufv.br

William Caires Silva Amorim
Department of Electrical Engineering
CEFET - MG
Belo Horizonte, MG, Brazil
william.caires@ufv.br

Matheus Pereira Silva
Department of Electrical Engineering
Federal University of Viçosa - UFV
Viçosa, MG, Brazil
matheus.p.silva10@gmail.com

Heverton Augusto Pereira
Department of Electrical Engineering
Federal University of Viçosa - UFV
Viçosa, MG, Brazil
heverton.pereira@ufv.br

***Abstract*—Solar irradiance is a fundamental component for the conversion of solar energy, since it expresses the potential to generate energy in a certain area of the earth's surface. Thus, understanding the irradiance levels of a certain place is essential to determine the solar generation potential. The most used incidence irradiance meters are: thermopile pyranometer, photodiode and pyrheliometer. Although these sensors measure with a high sensitivity, they present high costs of acquisition, as well as of maintenance. Thus, photosensitive technologies such as Light Dependent Resistor (LDR) sensors may be alternatives to these instruments. Therefore, a low-cost project with measures compatible with conventional solar irradiance meters is proposed in this work. A calibration of the LDR sensors will be done, based on a photodiode pyranometer. Thus, statistical analyzes of regressions between the collected points are done from the data collected via datalogger. Different values of resistance in the acquisition circuit, indicate better readings for different ranges of solar irradiance. The results show the validity of the system based on statistical analyzes performed through relative errors and correlation.**

***Index Terms*—Solar irradiance meter, LDR sensor, pyranometer, Arduino.**

I. INTRODUCTION

Solar irradiance is the designation given to the power emitted by the sun per unit of area, in particular that is transmitted in the form of electromagnetic radiation. This is an important variable to be considered in the orientation of projects that consider solar energy, such as: in meteorological research, remote sensing, buildings natural lighting and in the energy sector for the correct sizing of power capture system [1].

According to [2], measurements taken with satellites show that extraterrestrial solar irradiance is very stable and has an approximate value of 1366 W/m^2, at a Sun-Earth distance equal to 1 AU (astronomical unit), equivalent to 149,598,106 km. However, the external solar irradiance to the planet is attenuated and ceases to be constant, when interacting with the atmosphere. This fact is due to the absorption and scattering of photons with the constituent matter of the atmosphere [3].

The authors would like to thank the Brazilian agencies CNPq, CAPES and FAPEMIG by funding.

As a countermeasure to the depletion of fossil fuels and aiming for a more sustainable world, many countries are increasing their use of renewable energy to produce electricity, such as solar electricity [4], [5]. Besides, as the production of solar energy is directly dependent on irradiance, the measurement of this variable is important for the development of solar energy capture projects [6]. Besides, the knowledge of the average behavior of the incidence solar irradiance allows to estimate the viability of a photovoltaic project to guarantee higher efficiency of production during the year in a determined region [7]. Therefore, it adds reliability by reducing economic risks and quality to solar systems, affecting the costs of the generated energy.

In order to determine the local incident irradiance, one option is to use modern features to monitor climatic elements [8]. Among these, it is possible to cite the electronic sensors used to collect solar irradiance data, such as the pyranometer, pyrheliometers and albedometers. These devices measure irradiance in W/m^2 being highly accurate and therefore expensive [4]. The high cost of the sensors has promoted interest in the development of alternative measuring instruments with lower cost. The Light Dependent Resistor (LDR) sensor appears as a viable option because its resistance varies according to the intensity of incident light.

Few studies in the literature propose alternatives of low cost for measurement of solar irradiance. Thus, this work presents the development of an alternative prototype for data measurement, processing and subsequent presentation of the local irradiance. Several procedures were performed: data collection by means of datalogger, separation in irradiance ranges, development of polynomial regressions, selection of models with higher statistical coefficients, algorithm implementation in the Arduino platform and model evaluation comparing with validation data.

This paper is outlined as follows: Section II provides a description about the sensors and strategies for data collection. Moreover, solar irradiance sensor design is presented in Section III. Section IV presents the results obtained with the sensor developed. Conclusions are stated in Section V.

II. Sensors and Strategies for Data Collection

The incident solar irradiance on the terrestrial surface presents a spatial and temporal variability associated with several mechanisms of interruption, as the emission of pollutants, the variation of the cloudiness and the concentration of aerosols. This implies that the measuring instruments must have sensitivity to detect all these variations, raising the precision requirements of the devices. In this way, the instrumentation sensors are detailed below.

A. Photodiode Pyranometer

Fig. 1 shows a generic photodiode pyranometer. This device is a stable sensor with a sensitivity degradation of less than 2 % per year [2]. It consists of a semiconductor cell as a sensor element that proportionally converts the solar irradiance into electric current. Generally, the pyranometer is used to measure total solar irradiance on the horizontal plane or to observe small irradiance fluctuations, since it has an optimal temporal response.

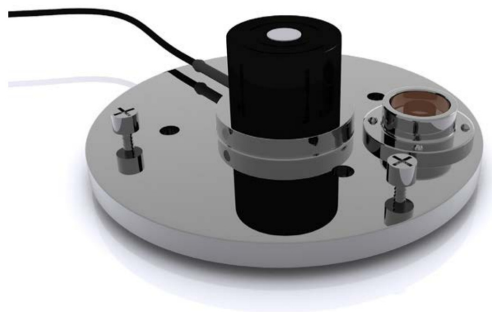

Fig. 1. Photodiode pyranometer sensor [2].

In addition, it is a robust and precise device, making it attractive for applications in meteorology and agrometeorology. Tab. I presents relevant characteristics of this sensor.

TABLE I
Photodiode pyranometer parameters.

Parameter	Typical Value
Sensitivity	90 μA per 1000 W/m^2
Stability	$< \pm$ 2 % change over a 1 year period
Response Time	10 μs
Temperature Dependence	0.15 % per $^{\circ}C$
Operating Temperature	-40 to $65^{\circ}C$
Size	2.38 cm Dia. $\times$ 2.54 cm H.
Weight	28 g
Cable Length	3.0 m

B. Light Dependent Resistor

This device is made of a cadmium sulphide or cadmium selenium cell which varies its resistance according to the incident light on its surface [9]. Therefore, the increase of incident light on the LDR surface causes a logarithmic decrease of the device resistance. Generally, the LDR resistance varies from 400 Ω (sunlight) to 1 MΩ (darkness) [4].

In order to verify if the LDR response to the incidence irradiance is satisfactory, it is necessary to analyze the spectrum of different commercial devices used for irradiance measurement and to compare them with the LDR spectrum, as shown in Fig. 2.

A sensor with good characteristics requires a response of 400 nm to 1200 nm, since 95 % of the solar energy is converted into that wavelength range. The comparison of the graphs of Fig. 2 reveals that the response of the thermocouple pyranometer is the most adequate, since it fills every spectrum. On the other hand, the photodiode pyranometer coincidently responds with the spectrum from 400 nm to 1200 nm, presenting itself as a good option of lower cost compared to the thermocouple pyranometer. Finally, the response spectrum of the LDR is within a range of 300 nm to 900 nm. Even with reduced wavelengths response, it is an extremely attractive device due to its low cost compared to other sensors.

C. Datalogger

Spider8 is a computer-based datalogger, capable of monitoring and recording information at high speed. It has simple installation, operation and configuration. It has eight channels, enabling data collection of eight variables simultaneously. The Spider8 has an integrated A/D converter and signal conditioner, which ensures system accuracy [11].

Four channels were used, one for each sensor. Each channel works with a separate 10-bit A/D converter, synchronized to ensure simultaneous measurements on all channels. After acquiring data by Spider8, they are handled by Catman, software installed on this equipment. The values of the sensors and the temporal variation of the measurements are presented in the form of Excel spreadsheets.

After the proper settings, the connections of the data acquisition circuit were made by connecting the pyranometer and the LDRs to the channels of the Spider8, as shown in Fig. 3.

The datalogger used was calibrated to measure voltage. Thus, it was necessary to use a 147 Ω resistor in parallel at the pyranometer output, according to the manufacturer's specifications. Besides, Spider8 has a 10-bit AD converter, with a pitch of 9.7 mV. To measure signals on the order of 15 mV (sensor output + 147 Ω adapter), the datalogger is not able to do it properly. Thus, an amplifier is needed to amplify the signal destined for the input of Spider8. The amplification gain used is given by:

$$|K| = \left| -\frac{R_2}{R_1} \right| = \frac{100k}{1k} = 100, \qquad (1)$$

where R_2 is the feedback resistor and R_1 is the input resistor on the inverter pin.

In addition, three LDR sensors are connected in series with different resistors (1 kΩ, 500 Ω and 100 Ω). Different resistors were used to increase the level of resolution according to the different ranges of incidence solar irradiance. The LDR sensor outputs are inserted into the datalogger to be measured.

After completing the previous steps, the equipment was installed at a 20° slope on a platform 22m high, whose coordinates are $20^{\circ}45^{'}49.32^{''}$ S and $42^{\circ}52^{'}4.08^{''}$ W, as shown in the Fig. 4. The data were collected during 5 days: November 23 to November 27, from 8:30 a.m. to 6:00 p.m., with sampling time equal to 2 min. In addition, the data from the first four days are used for model estimation, while the fifth day data is for validation.

According to the manufacturer's calibration certificate, the voltage signal on the pyranometer is converted directly into solar irradiance by:

$$12.44mV \leftrightarrow 1000W/m^2. \tag{2}$$

Therefore, each 12.44 mV at the pyranometer output is equal to 1000 W/m^2. Thus, the irradiance value G as a function of the pyranometer voltage V_{ref} is:

$$G = \frac{1000V_{ref}}{12.44 \times 10^{-3}\,|K|} = 803.86V_{ref}, \tag{3}$$

where G is given in W/m^2.

III. Solar Irradiance Sensor Design

The previous section details the obtaining of LDR voltage and solar irradiance data. This section is interested in the development of the LDR-based solar irradiance sensor.

There are two approaches to developing mathematical models: 1) based on process physics and 2) empirical. The first presupposes in-depth knowledge of the system, in addition the estimated parameters have physical meaning. On the other hand, the second generally does not have parameters with physical meanings. Furthermore, the main interest is to describe the response of the system, with few interest in the physical understanding of the process.

Nowadays, computer techniques optimize data processing, increasing interest in the development of empirical models. Thus, the focus of this paper is on polynomial empirical models (polynomial regression) based on the observation of the cause and effect relationship between input and output variables. Regression analysis is used as a descriptive method of data analysis. The $n-th$ order polynomial regression is given by:

$$\hat{y} = a_o + a_1x + a_2x^2 + \ldots + a_nx^n, \tag{4}$$

where a_i, $i = \{0, ..., n\}$, are the model coefficients, x is the LDR voltage and $\hat{y}$ is the estimated polynomial regression model.

A. Statistical Indexes for Model Analysis

For comparing data between the reference (pyranometer) and the device developed it is necessary to address statistical indexes. The coefficient of correlation (r) is used to study the behavior of two variables, i.e., it measures the degree of association between them. Thus, the r of the LDR voltage and the solar irradiance measured by the pyranometer is given by:

$$r_{xy} = \frac{\sqrt{\sum_{i=1}^{N}(x_i - \overline{x})(y_i - \overline{y})}}{\sqrt{\sum_{i=1}^{N}(x_i - \overline{x})^2 \sum_{i=1}^{N}(y_i - \overline{y})^2}}, \tag{5}$$

where $\overline{x}$ and $\overline{y}$ are the mean values of the data set collected for the LDR and pyranometer, respectively. Besides, N is the number of pairs of observations. The value of this coefficient is between -1 and +1. If there is no correlation between the variables, the coefficient is zero. A r value close to 1 indicates a positive correlation between the variables and a value close to -1 indicates a negative correlation [12]. The coefficient of correlation is not related with the quality of the model, therefore, another statistical index is needed.

The coefficient of determination (R^2) is used to evaluate the quality of the model, whose statistical function is to indicate how much the model is able to explain the system dynamics. In other words, it indicates how much the model can explain the observed values.

The R^2 varies between 0 and 1, and is expressed as:

$$R^2 = 1 - RMSE, \tag{6}$$

where $RMSE$ compares the estimated model with the mean time of the measured signal $\overline{y}$ and is given by [12]:

$$RMSE = \frac{\sqrt{\sum_{i=1}^{N}(y(k) - \hat{y}(k))^2}}{\sqrt{\sum_{i=1}^{N}(y(k) - \overline{y})^2}}, \tag{7}$$

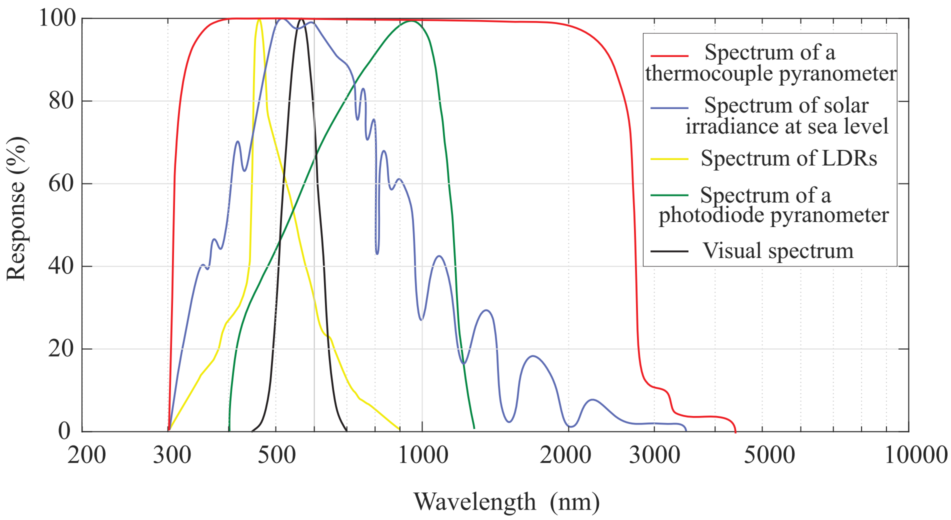

Fig. 2. Irradiance spectrum response of the sensors: photodiode pyranometer, thermocouple pyranometer and LDR; and of the solar irradiance at sea level. Adapted from [10].

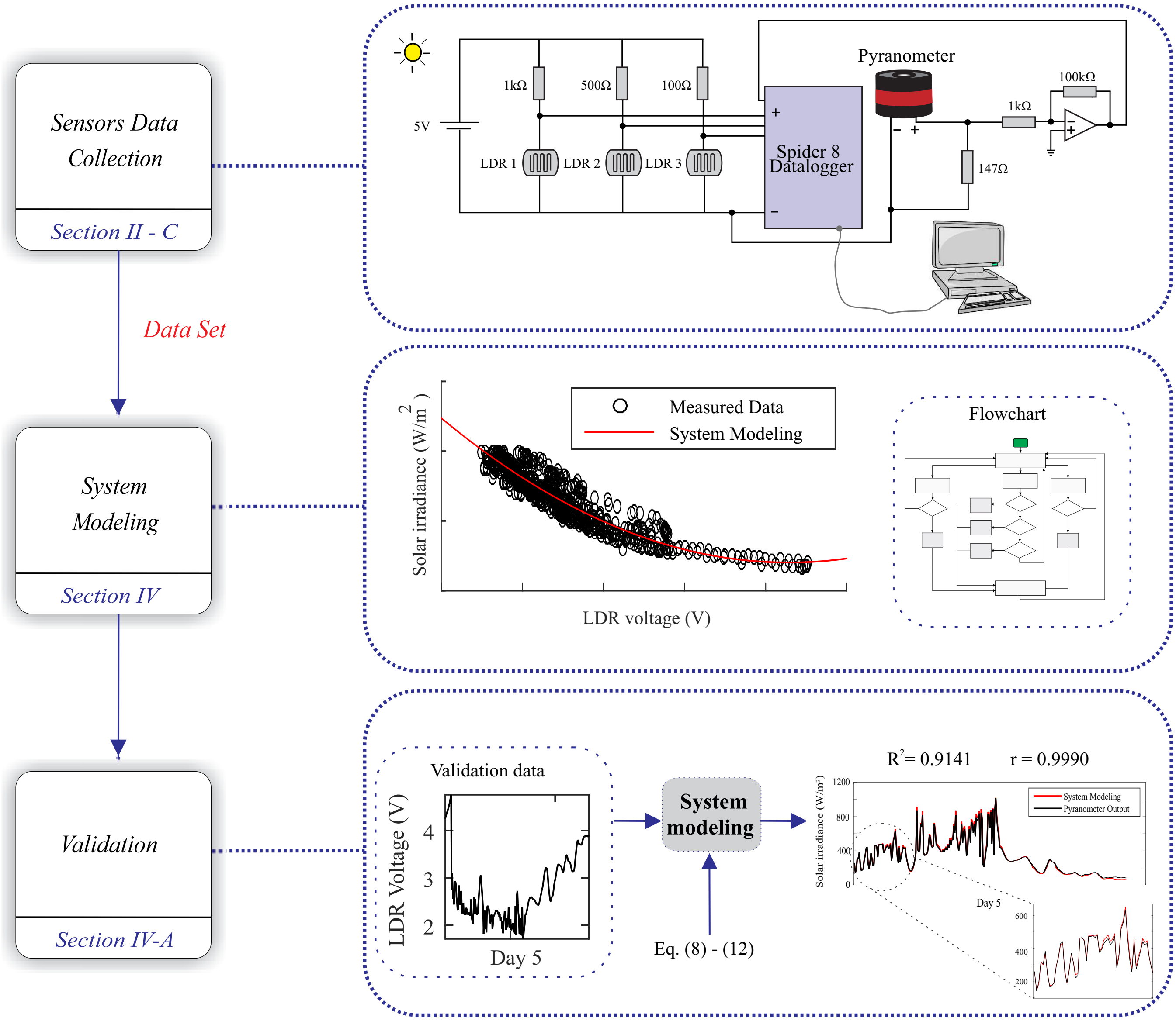

Fig. 3. Electrical schematic of the connections for data collection with pyranometer and LDRs.

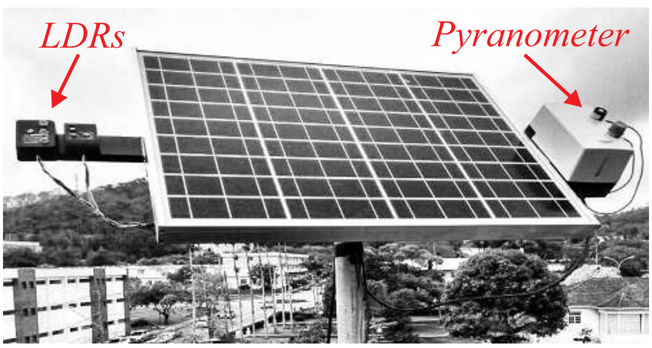

Fig. 4. Platform for data collection of LDRs and pyranometer sensors.

B. Arduino Uno Board

A microcontroller must be able to read and process the LDR voltage data and convert them to solar irradiance. The Arduino Uno board has been gaining strength in the market and has been a good compromise use it. The board is based on the ATmega328 microcontroller chip. Besides, it has 14 digital input/output pins, 6 analog inputs, a 16 MHz clock, a USB connection, a power outlet, an ICSP header, and a reset button. The communication with computers and another microcontroller has several facilities and was made via MODBUS RTU protocol [13].

The connection of the LDRs circuit with the Arduino was done through a serial interface, at a connection speed of 9600 bps.

IV. Development of the Solar Irradiance Sensor

For the five measurement days, Fig. 5 shows the voltage variation of the three LDRs connected to the 1 kΩ, 500 Ω and 100 Ω resistors. 1469 samples for each channel were obtained, resulting in a database of approximately 50 h. The data were divided into system modeling and validation, as shown in Fig. 5. The first 1209 samples were used for modeling and refer to Days 1-4, while the remaining 280 samples (Day 5) were used to validate the proposed models.

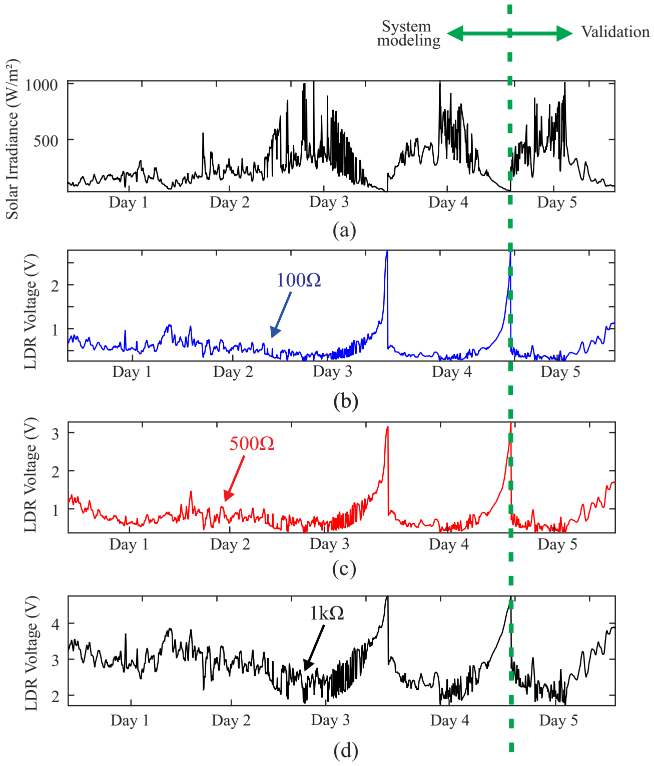

Fig. 5. (a) Solar irradiance 5-days profile. LDR voltage 5-days profile connected to the: (b) 100 Ω resistor. (c) 500 Ω resistor. (d) 1 kΩ resistor.

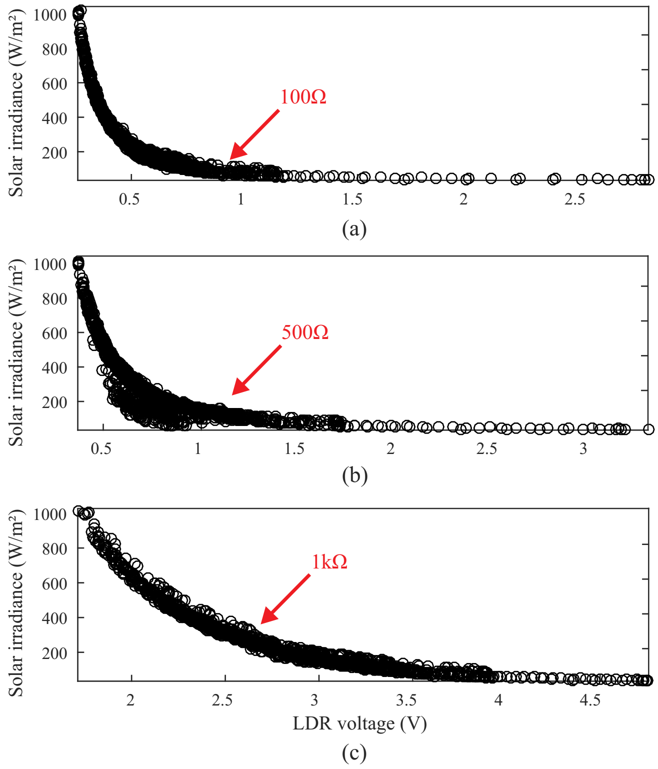

Fig. 6. Solar irradiance × LDR voltage connected to the (a) 100 Ω resistor. (b) 500 Ω resistor. (c) 1 kΩ resistor.

The pyranometer is used as a basis to determine the relationship between the LDR voltage (V) and solar irradiance (W/m^2). Besides, the LDR voltage sampling was performed synchronously with the reference sensor, allowing a direct analysis between the data collected by both components. Therefore, the LDR voltage and the respective local irradiance can be related as in Fig. 6.

From the results of Fig. 6, it is noticed that the LDR voltage range varies with different resistors connected. The voltage range is from 0.263 to 2.7848 V, 0.3702 to 3.2772 V and 1.7128 to 4.756 V for 100 Ω, 500 Ω and 1 kΩ, respectively. In addition, the curves are different in shape: Fig. 6(a) shows a higher rate of decrease than Fig. 6(b) and (c).

In order to obtain better results, an analysis for various solar irradiance intervals is proposed. Thus, the voltage data for Days 1-4 of each LDR were separated into the following irradiance ranges:

- Case I: 0 - 200 W/m^2;
- Case II: 200 - 400 W/m^2;
- Case III: 400 - 600 W/m^2;
- Case IV: 600 - 800 W/m^2;
- Case V: 800 - 1100 W/m^2.

Accordingly, 3 polynomial regressions were estimated for each case, resulting in 15 models (3 × 5). The model selection for the cases took into account the calculation of R^2 and r, as shown in Tab. II.

A comparison reveals that the 1 kΩ resistor model presented higher R^2 and r than the other models, for the Case I. For Cases II, III and IV, the 100 Ω resistor model presented better performance than the others. Similarly, the model with 500 Ω resistor for Case V. In addition, Tab. III shows the maximum and minimum LDR voltage value V_i, where $i = \{I, ..., V\}$, for the solar irradiance ranges.

TABLE II
DETERMINATION AND CORRELATION COEFFICIENTS FOR DEFINED SOLAR IRRADIANCE RANGES.

Case	100 Ω		500 Ω		1 kΩ	
	R^2	r	R^2	r	R^2	r
I	0.8632	-0.7364	0.5615	-0.7102	0.8689	-0.8945
II	0.9487	-0.9404	0.4926	-0.7147	0.9143	-0.9403
III	0.9468	-0.9676	0.9249	-0.9612	0.8015	-0.8803
IV	0.9527	-0.9726	0.9182	-0.9553	0.8458	-0.9056
V	0.7553	-0.8691	0.9421	-0.9602	0.8783	-0.3016

TABLE III
LDR VOLTAGE RANGE OF THE SELECTED MODELS FOR THE ANALYZED CASES.

LDR Voltage Range	Vi, i = {I,..,V}	
	min (V)	max (V)
Case I	2.75	4.76
Case II	0.38	0.61
Case III	0.32	0.39
Case IV	0.29	0.33
Case V	0.37	0.42

The flowchart of Fig. 7 presents graphically the algorithm developed for the logical and coherent sequence of data flow in the microcontroller. The LDR voltage are analyzed in real time, updating the output (solar irradiance), according to the read input value. Thus, the model in (8) is used for each voltage measurement cycle in the 2.75 V to 4.76 V range:

$$G_I = 47.5V_I^2 - 4.4 \times 10^2 V_I + 1048, \tag{8}$$

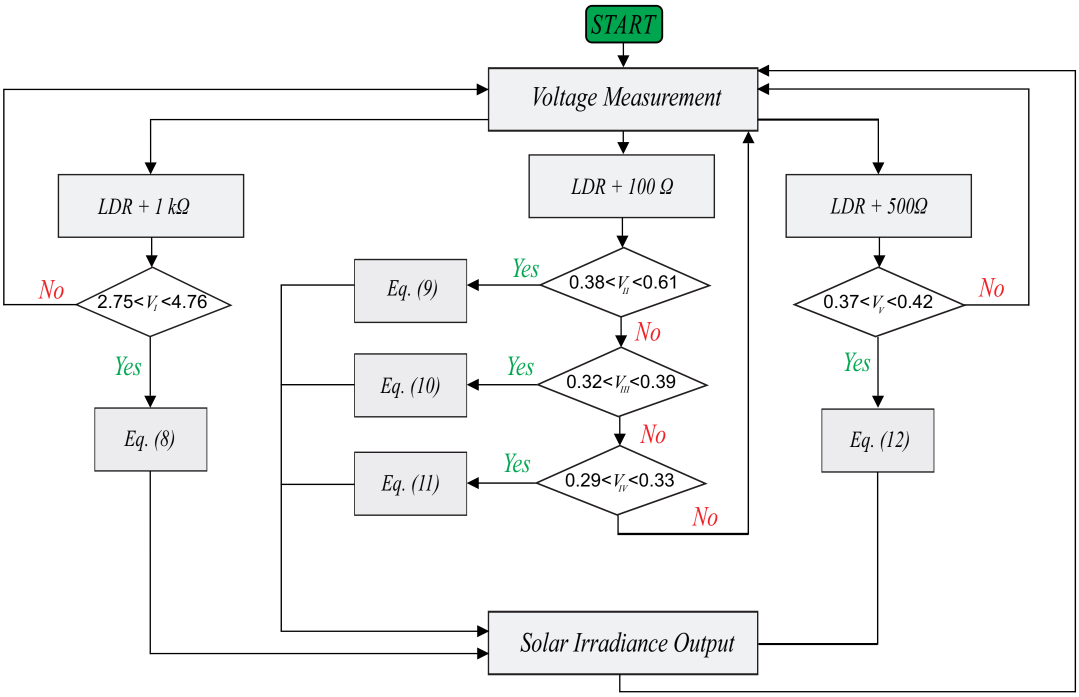

Fig. 7. Algorithm flowchart implemented to read LDR voltage and return the corresponding solar irradiance.

where G_I is the output in W/m^2 for the Case I.

When the voltage range of the LDR+100 Ω is between 0.38 and 0.61 V, the model (9) is used. Similarly, from 0.32 to 0.39 V and 0.29 to 0.33 V, the models corresponding to Cases III and IV are (10) and (11), respectively:

$$G_{II} = 5.5 \times 10^3 V_{II}^2 - 6.3 \times 10^3 V_{II} + 2 \times 10^3, \quad (9)$$

$$G_{III} = 1.93 \times 10^4 V_{III}^2 - 1.7 \times 10^4 V_{III} + 4 \times 10^3, \quad (10)$$

$$G_{IV} = 4.5 \times 10^4 V_{IV}^2 - 3.3 \times 10^4 V_{IV} + 6.5 \times 10^3, \quad (11)$$

where G_{II}, G_{III} and G_{IV} are the outputs for Cases II, III and IV.

Finally, if the LDR+500 Ω measured voltage is 0.37 to 0.42 V, the corresponding output model G_V is given by:

$$G_V = 4.8 \times 10^4 V_V^2 - 4.2 \times 10^4 V_V + 9999.7. \quad (12)$$

Fig. 8 shows the polynomial regressions with the highest value of R^2 and r for the analyzed solar irradiance ranges. From the results seen in Fig. 8 (a)-(e), the data collection was performed on days of low solar irradiance, with peaks of 1000 W/m^2 in few measurements. In other words, most of the data is concentrated in the region of 100 W/m^2 to 700 W/m^2. Thus, some considerations must be made:

- The sensor has a better solar irradiance estimation in the range of 100 W/m^2 to 700 W/m^2, since many collected points are in this interval;
- The number of points collected is small for 700 W/m^2 or more, affecting the quality of the database from these values;
- Extrapolating the ranges of the Cases impairs the measurement of irradiance by the LDRs, since the mathematical models have a specific voltage range for their application.

A. *Methodology Validation*

The polynomial regressions (8)-(12) were obtained for the modeling data. This methodology should be tested for another database, as shown in the schematic of Fig. 3.

The three LDRs voltage data of Day 5 are the inputs in the model obtained previously. The model output for these conditions is compared with the reference solar irradiance measurements and the R^2 and r coefficients are estimated, as shown in Tab. IV.

TABLE IV
R^2 AND r COEFFICIENTS FOR THE VALIDATION DATA.

Model	R²	r
Eq. (8)-(12)	0.9141	0.9990

The results show that the models (8)-(12) explain 91.41 % of the validation data. The measured results by the pyranometer and the LDR based system and the relative error between them, are presented in Tab. V. It is noticed that the relative error measurement is higher (6.26 % and 5.61 %) for the Case IV and V, because of the lack of samples in this range.

By means of (8) to (12) and the implemented algorithm, it was possible to obtain the LDR system solar irradiance of Day 5 and compare it with the pyranometer data, as shown in Fig. 9.

An error is observed between the two curves, however, the model dynamics is maintained when compared to the reference.

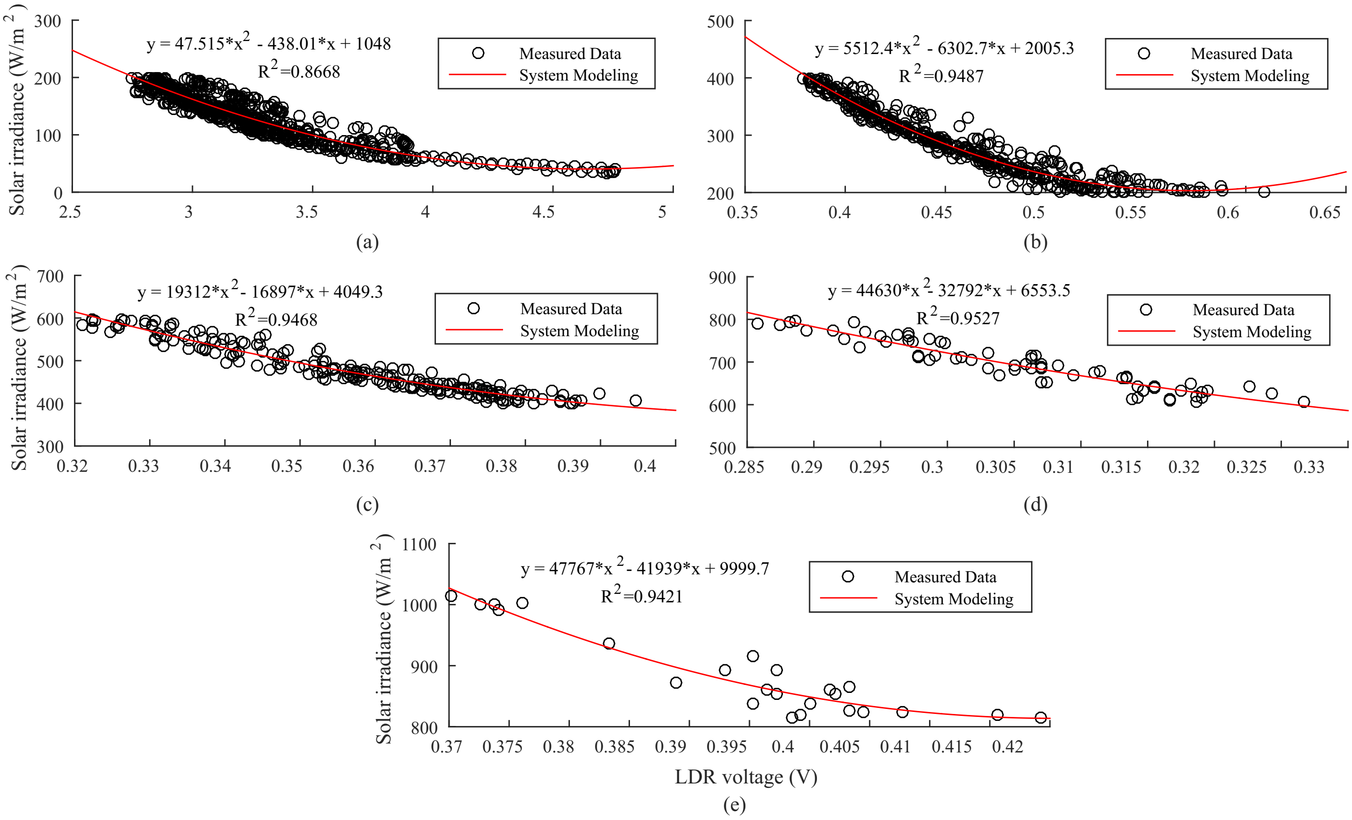

Fig. 8. Polynomial regression for Cases (a) I, (b) II, (c) III, (d) IV and (e) V, selected according to the coefficient of determination.

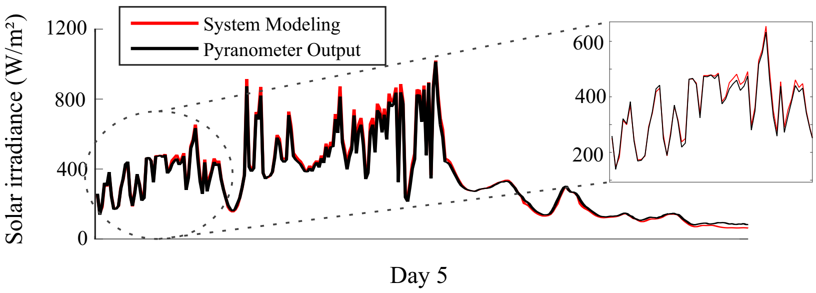

Fig. 9. Irradiance output read by the LDR after compiling the flowchart Fig. 7, compared to the reference for the validation data.

TABLE V
RELATIVE ERROR BETWEEN MEASUREMENTS PERFORMED WITH THE PYRANOMETER AND THE DEVELOPED SYSTEM.

Situation	Pyranometer (W/m²)	LDRs (W/m²)	Relative Error (%)
Case I	171.04	174.6	1.87
Case II	258.88	251.96	2.67
Case III	445.24	449.75	1.01
Case IV	617.27	695.93	6.26
Case V	838.30	885.30	5.61

V. CONCLUSION

The development of a low cost system for voltage data collection in LDRs and the presentation of the measured solar irradiance was provided in this work. The photodiode pyranometer was used as a reference to obtain a correspondence between its readings and the measured values of the acquisition circuit. In order to obtain the independent operation character of the irradiance meter, the Arduino platform was used to enable the data processing and feeding of the measurement circuits. This platform proved ideal for operation and construction of the meter.

The modeling methodology for each irradiance range was efficient for the climatic conditions of the days analyzed, according to the statistical indexes. In order to evaluate the proposals of this work, an analysis is made considering a database different from the data used for system modeling. The study revealed a R^2 fit of approximately 91% for the validation data. In addition, it was possible to observe a maximum relative error of 6 % between the system and reference measurements for the solar irradiance ranges evaluated.

As a proposal for continuity of this work, it may be possible to improve the system response by applying the oversampling/averaging to minimize the conversion noise, as well as propose a new data collection for more intense irradiance climatic conditions aiming to expand the operation range of the proposed sensor device.

REFERENCES

[1] R. J. dos Reis and C. Tiba. (2012, May) Atlas solarimetrico de minas gerais - vol. ii. Companhia Energetica de Minas Gerais. [Online]. Available: http://www.cemig.com.br/pt-br/A_Cemig_e_o_Futuro/inovacao/Alternativas_Energeticas/Documents/atlas_solarimetrico.pdf.

[2] C. E. de Minas Gerais Vol. I. (2012, May) Atlas solarimetrico de minas gerais. CEMIG. [Online]. Available: http://www.cemig.com.br/pt-br/A_Cemig_e_o_Futuro/inovacao/Alternativas_Energeticas/Documents/Atlas_Solarimetrico_CEMIG_12_09_menor.pdf.

[3] J. M. Wallace, *Atmospheric science : an introductory survey*. Amsterdam; Boston: Elsevier Academic Press, 2006.

[4] F. G. Hidalgo, R. F. Martinez, and E. Vidal, "Design of a low-cost sensor for solar irradiance," 2014, pp. 1–8.

[5] F. Martins, E. Pereira, and P. Edson, "Quality control of solar radiation data within sonda network in brazil: Preliminary results," in *ISES Conference Proceedings*, september 2014, pp. 1–9.

[6] A. H. Sabry, W. Z. W. Hasana, M. Z. A. A. Kadir, M. A. M. Radzi, and S. Shafie, "Low cost wireless sensor monitoring system for photovoltaic (pv) array parameters," in *2017 IEEE 4th International Conference on Smart Instrumentation, Measurement and Application (ICSIMA)*, Nov 2017, pp. 1–6.

[7] A. Zakariah, J. J. Jamian, and M. A. M. Yunus, "Dual-axis solar tracking system based on fuzzy logic control and light dependent resistors as feedback path elements," in *2015 IEEE Student Conference on Research and Development (SCOReD)*, Dec 2015, pp. 139–144.

[8] J. LATIMER, "Radiation measurement," in *National Research Council of Canada, Int. Field Year for the Great Lakes*, september 1971, p. 53.

[9] J. Cruz-Colon, L. Martinez-Mitjans, and E. Ortiz-Rivera, "Design of a low cost irradiance meter using a photovoltaic panel," in *Conference Record of the IEEE Photovoltaic Specialists Conference*, 06 2012, pp. 002 911–002 912.

[10] F. Martins, E. Pereira, S. Abreu, and R. Ruther. (2006, february) Brazil solar atlas. INPE. [Online]. Available: http://ftp.cptec.inpe.br/labren/publ/livros/brazil_solar_atlas_R1.pdf.

[11] Spider8 datasheet. HBM. [Online]. Available: http://www.hottinger.sk/Prospekty/Elektronika/IMT/Spider8/p_Spider8_e.pdf.

[12] L. A. Aguirre, *Introdução à Identificação de sistemas*, 3rd ed. Editora UFMG, 2007, vol. único.

[13] Arduino uno datasheet. [Online]. Available: https://datasheet.octopart.com/A000066-Arduino-datasheet-38879526.pdf.